

## COMPUTATION AND STABILITY OF PERIODIC ORBITS OF NONLINEAR MAPPINGS

Tassos C. Bountis<sup>1</sup>, Charalampos Skokos<sup>1,2</sup> and Michael N. Vrahatis<sup>3</sup>

<sup>1</sup>Department of Mathematics, Division of Applied Mathematics and  
Center of Research and Applications of Nonlinear Systems (CRANS),  
University of Patras, GR-26500, Patras, Greece

<sup>2</sup>Research Center for Astronomy, Academy of Athens,  
14 Anagnostopoulou str., GR-10673, Athens, Greece

<sup>3</sup>Department of Mathematics and  
University of Patras Artificial Intelligence Research Center (UPAIRC),  
University of Patras, GR-26110 Patras, Greece

**Keywords:** Symplectic maps, Periodic orbits, Topological Degree theory, Stability.

**Abstract.** *In this paper, we first present numerical methods that allow us to compute accurately periodic orbits in high dimensional mappings and demonstrate the effectiveness of our methods by computing orbits of various stability types. We then use a terminology for the different stability types, which is perfectly suited for systems with many degrees of freedom, since it clearly reflects the configuration of the eigenvalues of the corresponding monodromy matrix on the complex plane. Studying the distribution of these eigenvalues over the points of an unstable periodic orbit, we attempt to find connections between local dynamics and the global morphology of the orbit.*

### 1 INTRODUCTION

One of the most challenging problems facing nonlinear science today is the extension of our knowledge of low-dimensional dynamics to problems which involve several degrees of freedom. This is particularly true in the case of conservative systems (e.g. Hamiltonian systems or symplectic mappings), in which new and more complicated phenomena are expected in higher dimensions.

Hamiltonian systems with  $n \geq 2$  degrees of freedom have been studied extensively in the context of celestial mechanics, especially with regard to problems of galactic dynamics<sup>[1-5]</sup>. In such systems one of the most fruitful approaches is to examine the intersection of orbits with a  $2N(=2n-2)$ -dimensional Poincaré surface of section, on which the flow is reduced to a  $2N$ -dimensional symplectic mapping<sup>[6]</sup>.

Another very important application concerns the stability of particle beams in high energy hadron colliders, where symplectic mappings naturally arise e.g. due to periodically repeated (and of very brief duration) beam-beam collisions, or beam passage through magnetic focusing elements<sup>[7,8]</sup>.

Finding the periodic orbits of a dynamical system and determining their stability is a fundamental procedure in studying the behavior of the system. The stability (or instability) of a periodic orbit influences the dynamical behavior of nearby orbits. In particular, non-periodic orbits near a stable periodic orbit have a time evolution similar to the one exhibited by the periodic orbit, and so their behavior is said to be ordered, while in the neighborhood of an unstable periodic orbit the system is known to exhibit chaotic behavior.

In the present paper we present a numerical method for accurately locating periodic orbits, based on topological degree theory, and introduce a suitable terminology for the stability type of the computed periodic orbits. As an example, we apply the above method to a 4D symplectic map arising in particle beam dynamics.

### 2 CP- CRITERION

Many problems in different areas of science and technology lead to the study of the solutions of a system of nonlinear equations of the form:

$$F(X) = 0, \quad (1)$$

in an appropriate space. For example, these solutions can represent a set of equilibria for a dynamical system  $dX/dt = F(X)$ . Topological degree theory has been developed as a means of examining this solution set and obtaining information on their existence, their number as well as their nature. It is useful, for example, in bifurcation theory for providing information about the existence and stability of periodic solutions of ordinary differential equations as well as the existence of solutions of certain partial differential equations. Several of these applications involve the use of various fixed point theorems, which can be provided by means of the concept of the topological degree<sup>[9-15]</sup>.

Consider the problem of finding periodic orbits of period  $p$  of a flow in  $\mathbb{R}^{n+1}$ , by fixing one of the variables, say  $x_{n+1} = \text{const}$ , and locating points  $X^* = (x_1^*, x_2^*, \dots, x_n^*)$  on an  $n$ -dimensional surface of section  $\Sigma_{t_0}$  which satisfy the equation

$$\Phi^p(X^*) = X^*, \quad (2)$$

where  $\Phi^p = P_{t_0} : \Sigma_{t_0} \rightarrow \Sigma_{t_0}$  is the Poincaré map of the system. This is equivalent to finding fixed points in a  $2n$ -dimensional map. In other words we face the problem of solving the system  $F(X) = 0$ , with  $F = (f_1, f_2, \dots, f_n) = \Phi^p - I_n$ , where  $I_n$  is the  $n \times n$  identity matrix. It is well known that if we have a function  $F$ , which is continuous in an open and bounded domain  $D$  and the topological degree of  $F$  at  $0$  relative to  $D$  is not equal to zero, then there is at least one solution of the system  $F(X) = 0$  within  $D$ . This criterion can be used, in combination with the construction of a suitable  $n$ -polyhedron, called the *characteristic polyhedron*, for the calculation of a solution contained in this region.

This can be done as follows: Let  $M_n$  be the  $2^n \times n$  matrix whose rows are formed by all possible combinations of  $-1$  and  $1$ . Consider now an oriented  $n$ -polyhedron  $\Pi^n$ , with vertices  $V_k$ ,  $k=1, \dots, 2^n$ . If the  $2^n \times n$  matrix of signs associated with  $F$  and  $\Pi^n$ ,  $S(F; \Pi^n)$ , whose entries are the vectors

$$\text{sgn}F(V_k) = (\text{sgn}f_1(V_k), \text{sgn}f_2(V_k), \dots, \text{sgn}f_n(V_k)), \quad (3)$$

(where  $\text{sgn}$  denotes the well-known three valued sign function), is identical to  $M_n$ , possibly after some permutations of these rows, then  $\Pi^n$  is called the *characteristic polyhedron* relative to  $F$ . Furthermore, if  $F$  is continuous, then, under some suitable assumptions on the boundary of  $\Pi^n$

$$\text{deg}[F, \Pi^n, 0] = \sum_{X \in F^{-1}(0) \cap \text{int}(\Pi^n)} \text{sgn} \det J_F(X) = \pm 1 \neq 0, \quad (4)$$

implies the existence of a periodic orbit inside  $\Pi^n$ , where  $\text{deg}[F, \Pi^n, 0]$  denotes the topological degree of  $F$  at  $0$  relative to  $\Pi^n$ ,  $\text{int}(\Pi^n)$  determines the interior of  $\Pi^n$  and  $\det J_F(X)$  denotes the determinant of the Jacobian matrix at  $X$ .

To illustrate the characteristic polyhedron concept let us consider a function  $F = (f_1, f_2)$  in 2 dimensions. Each function  $f_i$ ,  $i=1,2$ , separates the space into a number of different regions, according to its sign, for some regions  $f_i < 0$  and for the rest  $f_i > 0$ ,  $i=1,2$ . Thus, in figure 1(a) we distinguish between the regions where  $f_1 < 0$  and  $f_2 < 0$ ,  $f_1 < 0$  and  $f_2 > 0$ ,  $f_1 > 0$  and  $f_2 > 0$ ,  $f_1 > 0$  and  $f_2 < 0$ . Clearly, the following combinations of signs are possible:  $(-, -)$ ,  $(-, +)$ ,  $(+, +)$  and  $(+, -)$ . Picking a point, close to the solution, from each region we construct a characteristic polyhedron. In this figure we can perceive a characteristic and a non-characteristic polyhedron  $\Pi^2$ . For a polyhedron  $\Pi^2$  to be characteristic all the above combinations of signs must appear at its vertices. Based on this criterion, polyhedron ABDC does not qualify as a characteristic polyhedron, whereas AEDC does.

Let us now describe the characteristic bisection method based on the above notion of the characteristic polyhedron, for the computation of periodic orbits. This method simply amounts to constructing another refined characteristic polyhedron, by bisecting a known one, say  $\Pi^n$ , in order to determine the solution with the desired accuracy. We compute the midpoint  $M$  of an 1-simplex, e.g.  $\langle V_i, V_j \rangle$ , which accounts for an one-dimensional edge of  $\Pi^n$ . The endpoints of this one-dimensional line segment are vertices of  $\Pi^n$ , for which the corresponding coordinates of the vectors,  $\text{sgn} F(V_i)$  and  $\text{sgn} F(V_j)$  differ from each other only in one entry. We call this a proper 1-simplex. To obtain another characteristic polyhedron  $\Pi_*^n$  we compare the sign of  $F(M)$  with that of  $F(V_i)$  and  $F(V_j)$  and substitute  $M$  for that vertex for which the signs are identical. Subsequently, we reapply the aforementioned technique to a different edge (for details we refer to [12,16,17]). In particular, let  $\langle V_i, V_j \rangle$  be a proper 1-simplex of  $\Pi^n$  and let  $B = (V_i + V_j)/2$  be its midpoint. We then distinguish the following three cases:

1. If the vectors  $\text{sgn} F(B)$  and  $\text{sgn} F(V_i)$  are identical then  $B$  replaces  $V_i$  and the process continues with the

- next proper 1-simplex.
2. If the vectors  $\text{sgn } F(B)$  and  $\text{sgn } F(V_j)$  are identical then B replaces  $V_j$  and the process continues with the next proper 1-simplex.
3. Otherwise the process continues with the next proper 1-simplex.

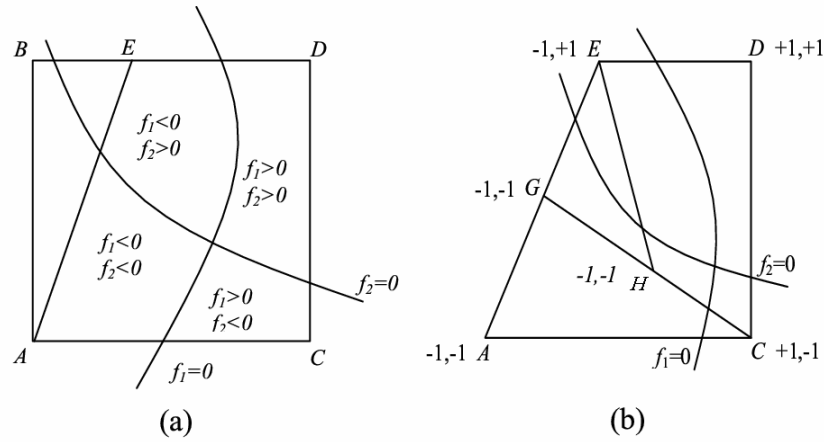


Figure 1. (a) The polyhedron ABDC is non-characteristic while the polyhedron AEDC is characteristic, (b) Application of the characteristic bisection method to the characteristic polyhedron AEDC, giving rise to the polyhedra GEDC and HEDC, which are also characteristic.

To fully appreciate the characteristic bisection method let us describe in figure 1(b), its repetitive operation on a characteristic polyhedron  $\Pi^2$ . Starting from the edge AE we find its midpoint G and then calculate its vector of signs, which is (-1,-1). Thus, vertex G replaces A and the new refined polyhedron GEDC, is also characteristic. Applying the same procedure, we further refine the polyhedron by considering the midpoint H of GC and checking the vector of signs at this point. In this case, its vector of signs is (-1,-1), so that vertex G can be replaced by vertex H. Consequently, the new refined polyhedron HEDC is also characteristic. This procedure continues up to the point that the midpoint of the longest diagonal of the refined polyhedron approximates the root within a predetermined accuracy.

Consider the characteristic n-polyhedron,  $\Pi^n$ , whose longest edge length is  $\Delta(\Pi^n)$ . The minimum number  $\zeta$  of bisections of the edges of  $\Pi^n$  required to obtain a characteristic polyhedron  $\Pi_*^n$  whose longest edge length satisfies  $\Delta(\Pi_*^n) \leq \varepsilon$ , for some accuracy  $\varepsilon \in (0,1)$ , is given by

$$\zeta = \lceil \log_2(\Delta(\Pi^n)\varepsilon^{-1}) \rceil. \quad (5)$$

Notice that  $\zeta$  is independent of the dimension n, implying that the bisection algorithm performs the same number of iterations as the bisection in one-dimension, which is optimal and asymptotically possesses the best rate of convergence [18]. The characteristic bisection method is efficient for low dimensions (say,  $n \leq 10$ ). This is due to the fact that the starting box as well as the characteristic polyhedron requires  $2^n$  vertices.

The characteristic bisection method has been applied to numerous difficult problems (see for example [19-23]). It is very useful in cases where the period of the periodic orbit is very high and especially when the orbit is unstable, since the method always converges within the initial specified region.

A further advantage of the characteristic bisection method is the convenient way with which we can distinguish the exact location of all periodic orbits of a given period, including the unstable orbits. This can be achieved through the coloring of the surface of section. The coloring process works as follows. Suppose that in a flow the periodic orbit under consideration is of period p. Denote the initial point by  $(x_0, \dot{x}_0)$ . We integrate the equations of motion, starting from  $(x_0, \dot{x}_0)$ , up to the point that the orbit intersects the x-axis  $2p$  times. Let  $(x, \dot{x})$  denote the point at the end of the integration. We evaluate the signs of the following differences:

$$(x - x_0) \quad \text{and} \quad (\dot{x} - \dot{x}_0). \quad (6)$$

Clearly, four combinations of signs are possible; namely (-,-), (-,+), (+,+) and (+,-) (see figure 2). Each one of these combinations corresponds to a different color. More specifically, starting from heavy gray to light gray we

colour the areas that correspond to the sign combinations  $(+,-)$ ,  $(-,-)$ ,  $(-,+)$  and  $(+,+)$ . To color the whole plane we select each point contained in the plane as the initial point and apply the coloring procedure. At each point where the four different colors meet, a periodic orbit (stable or unstable) exists.

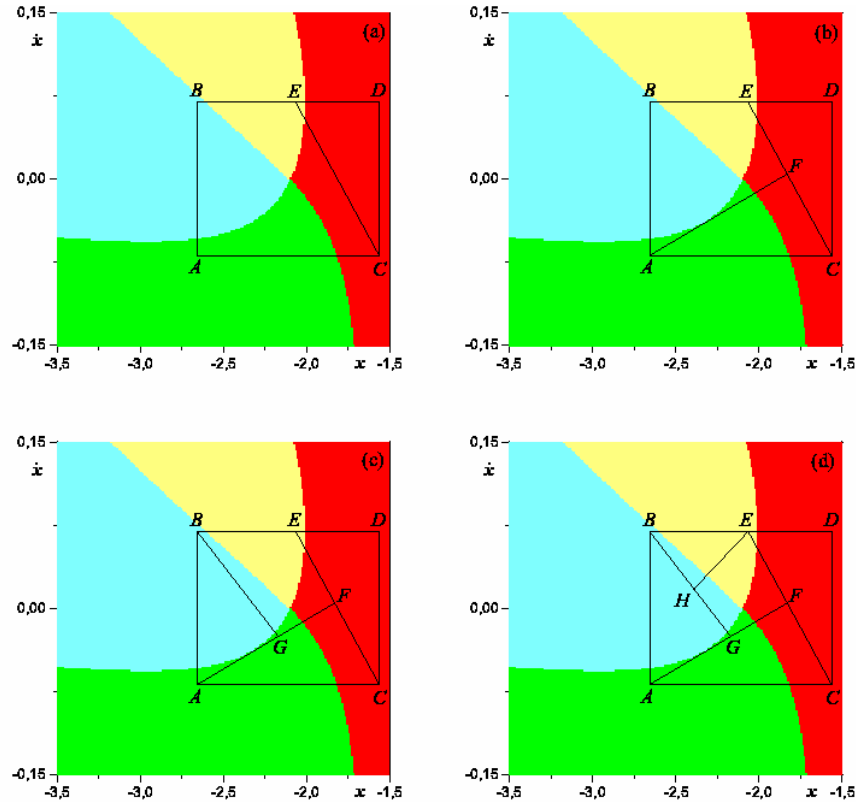


Figure 2. Application of the characteristic bisection method. Starting from heavy gray to light gray we color the areas that correspond to the sign combinations  $(+,-)$ ,  $(-,-)$ ,  $(-,+)$  and  $(+,+)$ .

In figures 2(a)-(d) the application of the characteristic bisection method is illustrated. Starting with a polyhedron  $ABDC$  (figure 2(a)), we examine whether it is characteristic or not. In the present case  $ABDC$  is not characteristic; this is easily verifiable by the fact that two vertices of the box have the same color. To overcome this problem, we need to determine a new vertex that will contain the missing combination; such a vertex is  $E$ . Having constructed a characteristic polyhedron we legitimately apply the method. In figure 2(b) we select the midpoint,  $F$ , of the largest edge, namely  $EC$ , and examine the corresponding combination of signs at  $F$ . Since the combination at  $F$  is identical to that in  $C$  (these two points have the same color),  $F$  substitutes  $C$  giving rise to a new refined characteristic polyhedron,  $ABEF$ . Figures 2(c), (d) exhibit two subsequent iterations of this method. Both  $GBEF$  and  $GHEF$  are characteristic. Following this procedure the desired solution is successfully captured.

Of course, the application of the characteristic bisection method does not necessarily require the coloring procedure. We utilized this procedure to illustrate the operation of the method and to provide a visualization of the solution.

### 3 STABILITY TYPES OF PERIODIC ORBITS

The linear stability or instability of a periodic orbit of an  $n+1$  degrees of freedom Hamiltonian flow is determined by the eigenvalues of the corresponding  $2n \times 2n$  monodromy matrix (see for example [24, 25]). This is a matrix whose columns are suitably chosen linearly independent solutions of the *variational equations*, which describe the time evolution of a small deviation from the periodic orbit. Equivalently the linear stability of a periodic orbit of  $2n$ -dimensional symplectic map is determined by the eigenvalues of the  $2n \times 2n$  return Jacobian matrix [26, 27, 13]. We note that for the above systems if  $\lambda$  is an eigenvalue then  $1/\lambda$  is also an eigenvalue, and if  $\lambda$  is an eigenvalue the complex conjugate  $\lambda^*$  is also an eigenvalue. All the different stability cases are shown in figure 3. The orbit is stable (S) when  $\lambda$  and  $1/\lambda$  are complex conjugate numbers on the unit circle. The orbit is unstable (U) when  $\lambda$  and  $1/\lambda$  are real (both positive or negative). The orbit is complex unstable ( $\Delta$ ) when we have four complex eigenvalues not lying on the unit circle and the real axis, forming two pairs of inverse numbers and two pairs of complex conjugate numbers. Two of the eigenvalues are inside the unit circle while the other two are outside it.

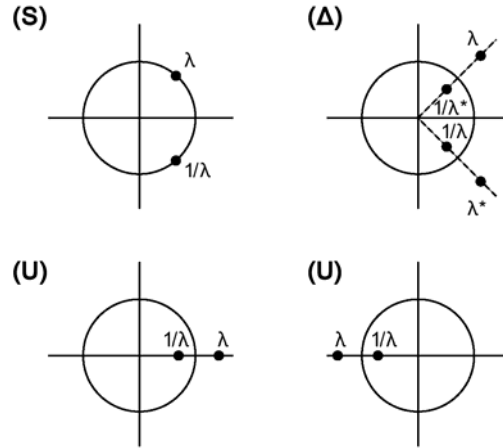


Figure 3. Configuration of the eigenvalues of the monodromy matrix on the complex plane, with respect to the unit circle, for the stable (S), unstable (U) and complex unstable ( $\Delta$ ) cases. We note that  $\lambda^*$  denotes the complex conjugate of  $\lambda$ .

The general stability type of a periodic orbit of a Hamiltonian system with  $n+1$  degrees of freedom, or of a  $2n$ -dimensional symplectic map is <sup>[25]</sup>

$$S_k U_m \Delta_l, \quad (7)$$

where  $k$ ,  $m$  and  $l$  are integer numbers, denoting that  $2k$  eigenvalues are on the unit circle,  $2m$  eigenvalues are on the real axis and  $4l$  eigenvalues are on the complex plane but not on the unit circle and the real axis. The integers  $k$ ,  $m$ ,  $l$  satisfy the inequalities:

$$0 \leq k \leq n, \quad 0 \leq m \leq n, \quad 0 \leq l \leq [n/2] \quad (8)$$

and the constraint

$$k + m + 2l = n. \quad (9)$$

In the case of 4-dimensional maps (an example of which is studied in the next section) or 3 degrees of freedom Hamiltonian systems, the periodic orbits can exhibit 4 different stability types according to equations (7)-(9); namely  $S_2$ ,  $S_1 U_1$ ,  $U_2$  and  $\Delta_1$ .

#### 4 PERIODIC ORBITS OF A 4-DIMENSIONAL SYMPLECTIC MAP

As an example, we shall apply our method to the periodic orbits of the 4-dimensional symplectic map

$$T : \begin{pmatrix} x'_1 \\ x'_2 \\ x'_3 \\ x'_4 \end{pmatrix} = \begin{pmatrix} \cos \omega_1 & -\sin \omega_1 & 0 & 0 \\ \sin \omega_1 & \cos \omega_1 & 0 & 0 \\ 0 & 0 & \cos \omega_2 & -\sin \omega_2 \\ 0 & 0 & \sin \omega_2 & \cos \omega_2 \end{pmatrix} \times \begin{pmatrix} x_1 \\ x_2 + x_1^2 - x_3^2 \\ x_3 \\ x_4 - 2x_1 x_3 \end{pmatrix}, \quad (10)$$

which describes the instantaneous effect experienced by a hadronic particle as it passes through a magnetic focusing element of the FODO cell type <sup>[7, 13, 14]</sup>.  $x_1$  and  $x_3$  are the particle's deflections from the ideal (circular) orbit, in the horizontal and vertical directions respectively, and  $x_2$ ,  $x_4$  are the associated 'momenta', while  $\omega_1$ ,  $\omega_2$  are related to the accelerator's betatron frequencies (or 'tunes')  $q_x$ ,  $q_y$  by

$$\omega_1 = 2\pi q_x, \quad \omega_2 = 2\pi q_y \tag{11}$$

and constitute the main parameters that can be varied by an experimentalist.

Using  $q_x=0.28$  and  $q_y=0.31$ , we have succeeded in computing periodic orbits for periods  $p$  up to the thousands, within an accuracy of  $\epsilon=10^{-15}$ . This means that

$$\|T^p(X^*) - X^*\| \leq \epsilon, \tag{12}$$

where  $\| \cdot \|$  denotes the Euclidean norm and  $X^*$  is the initial conditions array of the periodic orbit. In table 1 we list some of these orbits, giving also their initial conditions and indicating their stability type.

Period	S.T.	$x_1$	$x_2$	$x_3$	$x_4$
29(a)	$S_2$	.054115471909559	.033452533896669	.123803811258383	.302891822631234
29(b)	$S_1U_1$	.053714958340646	-.021127423014299	.126599277466037	-.288382572209036
29(c)	$S_1U_1$	-.311914175003230	.478963436888487	.072275663783410	.000149103204147
29(d)	$S_1U_1$	-.426820469769928	-.696514992607285	.271814834256359	-.402734706275434
29(e)	$U_2$	.467606951226090	.287263398595477	-.060318149783338	-.055560910967235
29(f)	$\Delta_1$	.391491732796431	.275189221962443	-.072683249141786	-.120237601901905
1110	$S_2$	.043655915204738	-.085080231465811	-.024179438643791	-.045566874737762
1110	$S_1U_1$	.397170936606918	-.181703664251662	.008899847771039	.066503595515161
1110	$U_2$	.337621956752420	.159497127557947	-.025276553445374	-.083066394306752
3427	$S_2$	.015138176638644	-.007636910751599	.027195105687227	.357893918903753
3427	$S_1U_1$	-.337639441332020	.029662641196283	-.167198400130657	.060223832997082
3427	$\Delta_1$	-.033187545699040	-.064807782377702	-.022594721878829	-.065664313143049
33092	$S_1U_1$	-.080099355622269	-.097941671799252	-.117764715099814	-.000246950450343
33092	$U_2$	-.420430408039337	.167141448638504	.214758833536393	-.036705323743372
33092	$\Delta_1$	.182805145505144	-.088673776696611	-.166727694831605	-.133587268367562
34202	$S_1U_1$	-.441846803970965	-.508725462305463	.057087631646123	-.027426076281871
34202	$U_2$	.197533223112076	-.182875153056365	-.144625557529287	-.082872892401335
34202	$\Delta_1$	-.108426091566732	-.050257267184845	-.134364519937652	.062300085029408
37629	$U_2$	-.468552017011198	-.604027173874510	-.015514258102956	.010180985462038
37629	$\Delta_1$	-.378873134810995	-.359329069465166	-.020965908282744	.013681842094073

Table 1. Initial conditions  $x_1, x_2, x_3, x_4$  of periodic orbits and their stability type (S.T.). The periodic orbits of period 29 are named with letters from a to f.

The dynamical behavior of orbits in different regions of phase space is influenced strongly by the properties of the nearby periodic orbits. In figure 4 we see the distribution of the six periodic orbits of period 29 listed in table 1, as 29(a) to 29(f). We note that only orbit 29(a), located near the origin and marked by small crosses in figure 4(b), is stable, with all 4 of its complex eigenvalues on the unit circle.

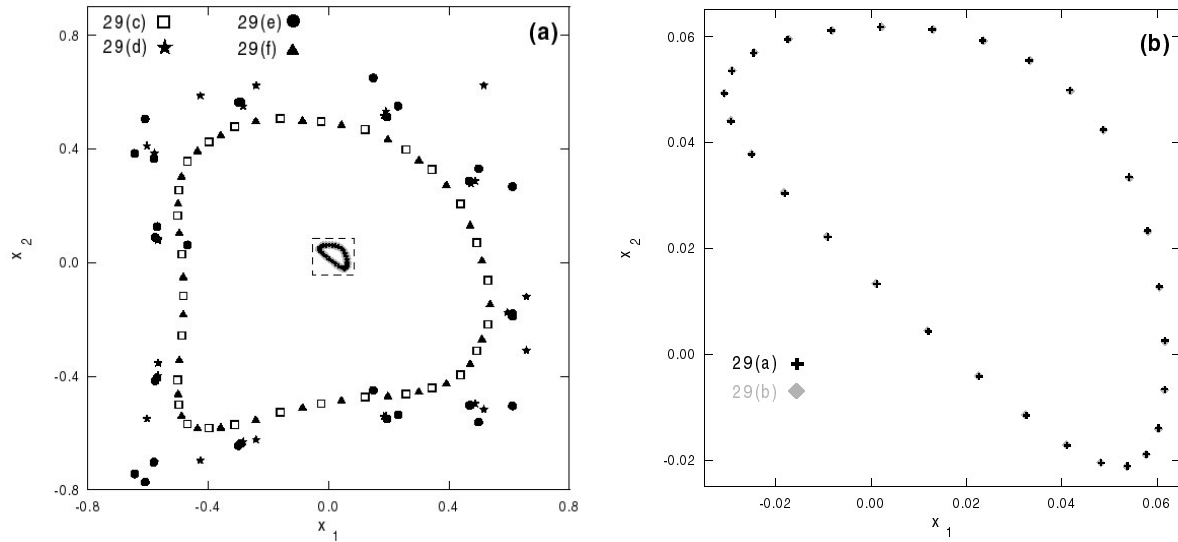


Figure 4. (a) Projection on the  $x_1x_2$  plane of the six periodic orbits of period 29 listed in table 1. The points of each orbit are marked by different symbols. (b) Enlargement of the region included in the dashed-line frame of (a), where the points of the periodic orbits 29(a) and 29(b) are located. Note that the points of the two orbits are located very close to each other in this projection.

The orbit 29(b), on the other hand, whose points are located very close to the ones of orbit 29(a) in figure 4(b), is slightly chaotic since its stability type is  $S_1U_1$  and the norm of the larger real eigenvalue is  $|\lambda|=1.00000001451116$ . The points of the orbit generated by perturbing the initial conditions of the unstable orbit 29(b) by  $dx_1=+0.003$ , form the ordered structure plotted in figure 5. On the other hand the orbit we get by perturbing the initial condition of the  $S_1U_1$  type orbit 29(c) by  $dx_2=+0.025$ , exhibits chaotic behavior since its points are scattered in a region located nearby the 29(c) orbit and finally escape to infinity after about 32,000 iterations (figure 6). We note that orbits 29(c) has the same stability type as 29(b); i.e.  $S_1U_1$  but the norm of its larger real eigenvalue is  $|\lambda|=1.20719498710467$ . The perturbed orbit of figure 6 is influenced by the nearby unstable orbit 29(f) whose stability type is  $\Delta_1$ , as well as by the other two unstable orbits 29(d) and 29(e).

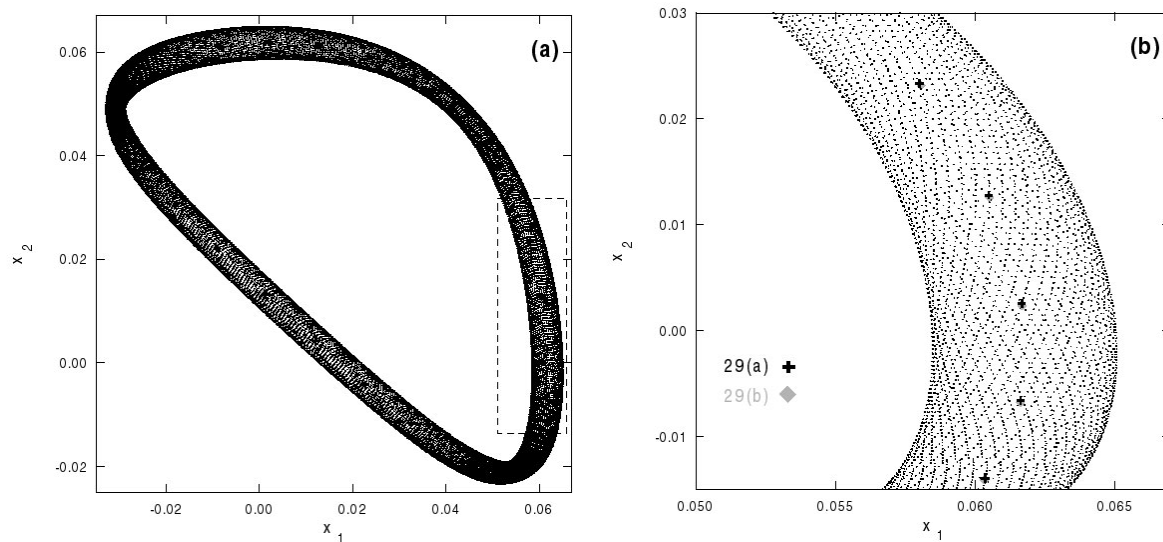


Figure 5. (a) Projection on the  $x_1x_2$  plane of the orbit whose initial conditions are generated by perturbing the initial conditions of orbit 29(b) by  $dx_1=+0.003$ . (b) Enlargement of the region included in the dashed-line frame of (a). Some points of the orbits 29(a) and 29(b) are also visible.

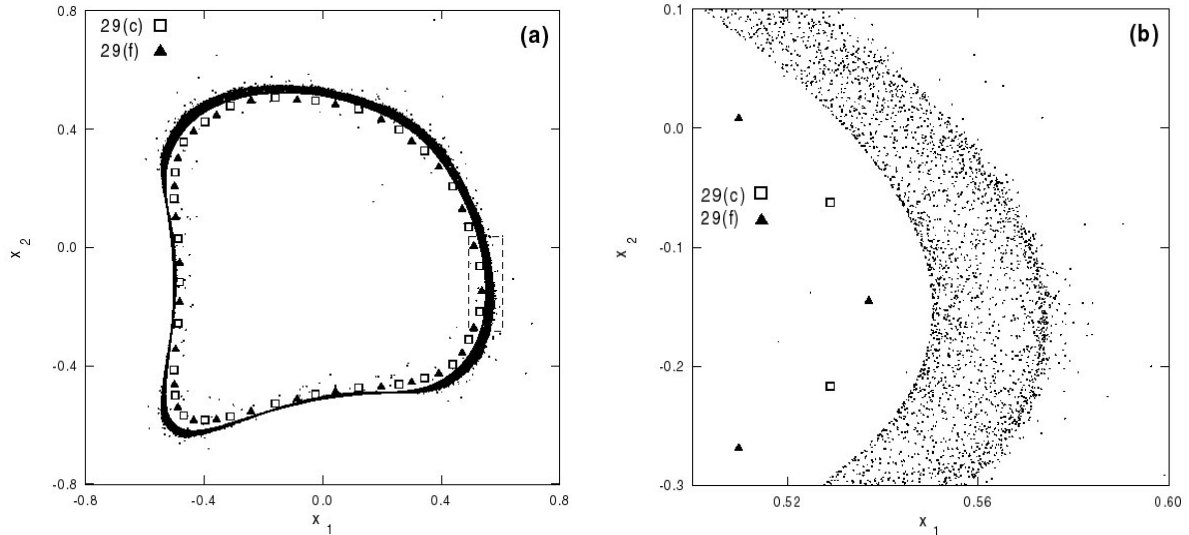


Figure 6.(a) Projection on the  $x_1x_2$  plane of the orbit whose initial conditions are generated by perturbing the initial conditions of orbit 29(c) by  $dx_2=+0.025$ . (b) Enlargement of the region included in the dashed-line frame of (a). Some points of the orbits 29(c) and 29(f) are also visible.

## 5 CONCLUSIONS

In this paper we have described an efficient method for rapidly and accurately computing periodic orbits in dynamical systems, which we call the characteristic bisection method. We have applied our method to a 4-dimensional symplectic mapping of interest to accelerator dynamics and succeeded in finding periodic orbits of very high period and of various stability types.

It is important to note that in such  $2N$ -dimensional conservative dynamical systems, the study of stability is a subtle matter, as it involves  $N$  (generally complex) eigenvalue pairs, whose computation requires a very accurate knowledge of the periodic orbit itself. Stability is expected to be the exception rather than the rule, since it demands that all eigenvalue pairs lie on the unit circle.

Now, as some parameter of the problem is varied, one (or more) eigenvalue pairs begin to "collide" and split off the unit circle rendering the orbit unstable. This raises the need for different notation in order to distinguish among all these stability types, according to their number of eigenvalues whose magnitude is larger than 1. For this reason, we introduced such a notation in section 3 and then used it to characterize, as an example, all different period 29 orbits of the 4-dimensional map (10).

The next step in this study is, of course, the examination of the connection between all these different types of instability and the complexity of the dynamics in the vicinity of the corresponding periodic orbits. It is reasonable to expect that, as the number of eigenvalues exiting the unit circle increases (and the orbit becomes "more unstable") the motion in the neighborhood of the orbit would exhibit a higher degree of chaotic behavior.

Thus, since we have developed in our work reliable quantitative criteria, by which one can study and compare chaotic vs. regular dynamics in phase space <sup>[8, 13, 14, 25, 28]</sup>, it is our next target to address these questions and present our results in a future publication.

## ACKNOWLEDGEMENTS

Ch. Skokos was supported by "Karatheodory" post-doctoral fellowship No 2794 of the University of Patras and by the Research Committee of the Academy of Athens (program No 200/532).

## REFERENCES

- [1] Hénon M. and Heiles C. (1964), "The applicability of the third integral of the motion: Some numerical experiments", *Astron. J.*, 69, pp. 73-79.
- [2] Contopoulos G, Magnenat P. and Martinet L. (1982), "Invariant surfaces and orbital behaviour in dynamical systems of 3 degrees of freedom", *Physica D*, 6, pp. 126-136.
- [3] Contopoulos G and Magnenat P. (1985). "Simple three-dimensional periodic orbits in a galactic type potential", *Celest. Mech.*, 37, pp. 387-414.
- [4] Skokos Ch., Patsis P. A. and Athanassoula E. (2002), "Orbital dynamics of three-dimensional bars: I. The backbone of 3D bars. A fiducial case", *MNRAS*, in press.
- [5] Skokos Ch., Patsis P. A. and Athanassoula E. (2002), "Orbital dynamics of three-dimensional bars: II. Investigation of the parameter space", *MNRAS*, in press.
- [6] Lichtenberg A. J. and Leiberman M. A. (1983), *Regular and Stochastic Motion*, Applied Mathematical Sciences 38, Springer-Verlag, New York.
- [7] Bountis T. C. and Tompaidis S. (1991), "Strong and weak instabilities in a 4D mapping model of FODO cell dynamics", *Future Problems in Nonlinear Particle Accelerators*, eds. Turchetti G. and Scandale W., World Scientific, Singapore, pp. 112-127.
- [8] Bountis T. C. and Kollmann M. (1994). "Diffusion rates in a four-dimensional mapping model of accelerator dynamics", *Physica D*, 71, pp. 122-131.
- [9] Cronin J. (1964), *Fixed points and topological degree in nonlinear analysis*, Mathematical Surveys No. 11, Amer. Math. Soc., Providence, Rhode Island.
- [10] Lloyd N. G. (1978), *Degree Theory*, Cambridge University Press, Cambridge.
- [11] Vrahatis M. N. (1989), "A short proof and a generalization of Miranda's existence theorem", *Proc. Amer. Math. Soc.*, 107, pp. 701-703.
- [12] Vrahatis M. N. (1995), "An efficient method for locating and computing periodic orbits of nonlinear mappings", *J. Comp. Phys.*, 119, pp 105-119.
- [13] Vrahatis M. N., Bountis T. C. and Kollmann M. (1996), "Periodic orbits and invariant surfaces of 4-D nonlinear mappings", *Inter. J. Bifurc. Chaos*, 6, pp. 1425-1437.
- [14] Vrahatis M.N., Isliker H. and Bountis T. C. (1997), "Structure and breakdown of invariant tori in a 4-D mapping model of accelerator dynamics", *Inter. J. Bifurc. Chaos*, 7, pp. 2707-2722.
- [15] Mourrain B., Vrahatis M. N. and Yakoubsohn J. C. (2002), "On the complexity of isolating real roots and computing with certainty the topological degree", *J. Complexity*, in press.
- [16] Vrahatis M.N. (1988), "Solving systems of nonlinear equations using the nonzero value of the topological degree", *ACM Trans. Math. Software*, 14, pp. 312-329.
- [17] Vrahatis M.N. (1988), "CHABIS: A mathematical software package for locating and evaluating roots of systems of nonlinear equations", *ACM Trans. Math. Software*, 14, pp. 330-336.
- [18] Sikorski K. (1982), "Bisection is optimal", *Numer. Math.*, 40, pp.111-117.
- [19] Drossos L., Ragos O., Vrahatis M. N. and Bountis T. C. (1996), "Method for computing long periodic orbits of dynamical systems", *Phys. Rev. E*, 53, pp.1206-1211.
- [20] Waalkens H., Wiersig J. and Dullin H. R.(1997), "Elliptic quantum billiard", *Annals Phys.* 260, pp. 50-90.
- [21] Buric N. and Mudrinic M., (1998), "Modular smoothing of action", *J. Phys. A*, 31, pp. 1875-1892.
- [22] Kalantonis V. S., Perdios E. A., Perdiou A. E. and Vrahatis M. N. (2001), "Computing with certainty individual members of families of periodic orbits of a given period", *Cel. Mech. Dyn. Astron.*, 80, pp. 81-96.
- [23] Vrahatis M. N., Perdiou A. E., Kalantonis V. S., Perdios E. A., Papadakis K., Prosmiiti R. and Farantos S. C. (2001), "Application of the characteristic bisection method for locating and computing periodic orbits in molecular systems", *Comp. Phys. Comm.*, 138, pp.53-68.
- [24] Yakubovich V. A and Starzhinskii V. M. (1975), *Linear Differential Equations with Periodic Coefficients*, Vol. 1, J. Wiley, New York.
- [25] Skokos Ch. (2001), "On the stability of periodic orbits of high dimensional autonomous Hamiltonian systems", *Physica D*, 159, pp. 155-179.
- [26] Greene J. M. (1979), "A method for determining a stochastic transition", *J. Math. Phys.*, 20, pp. 1183-1201.
- [27] Bountis T. C. and Helleman R. H. G. (1981), "On the stability of periodic orbits of two-dimensional mappings", *J. Math. Phys.*, 22, 1867-1877.
- [28] Skokos C., Antonopoulos C., Bountis T. and Vrahatis M.N., "Smaller Alignment Index(SALI): Detecting Order and Chaos in Conservative Dynamical Systems", to appear in the Proceedings of the 4<sup>th</sup> GRACM Congress in Comp. Mechanics, Patras (2002).